A Mathematical Model to Investigate Gain-Induced Oscillation in the Human Cardiovascular System

Dontwi, I. K.
Department of Mathematics, Kwame Nkrumah University of Science & Technology, Kumasi, Ghana

Appiah, S. T.
Department of Mathematics, University of Mines and Technology, Tarkwa, Ghana

Boateng, F. O.
Department of Information Technology Education, University of Education, Winneba, Kumasi, Ghana

Asiedu-Addo, S. K.
Department of Mathematics Education, University of Education Winneba, Ghana

Abstract

"Mayer waves" are long-period (6 to 12 seconds) oscillations in arterial blood pressure, which have been observed and studied for more than 100 years in the cardiovascular system of humans and other mammals. A mathematical model of the human cardiovascular system is presented, incorporating parameters relevant to the onset of Mayer waves. The model is analyzed using methods of Lyapunov stability and Hopf bifurcation theory. The analysis shows that increase in the gain of the baroreflex feedback loop controlling venous volume may lead to the onset of oscillations, while changes in the other parameters considered do not affect stability of the equilibrium state. The results agree with observations of Mayer waves in human subjects, both in the period of the oscillations and in the observed age-dependence of Mayer waves. This leads to a proposed explanation of their occurrence, namely that Mayer waves are a "gain-induced instability".

Introduction

The existence of fluctuations in blood pressure has been known since the introduction of the recording manometer by C. Ludwig, (Penaz and Mayer, 1978). These fluctuations, usually referred to as waves, are classified by various methods including the name of the discoverer, the origin, physiological cause, or the frequency or period. The term Mayer waves refers to periodic fluctuations in blood pressure which are slower than respiration in animals with normal respiratory movements. They were announced by S. Mayer and hence the name. They are also known as third order waves. The frequencies reported by various authors for Mayer waves differ considerably. Those described by Mayer in rabbits had a frequency of 6-9 waves/min., while other researchers have found waves with frequencies ranging from 7-12 waves/min. in humans (Penaz and Mayer, 1978).

Some researchers have proposed to designate these waves as the "10-second-rhythm" (see for example Penaz and Mayer, 1978). The onset of Mayer waves may result in serious physiological implications, such as fainting. Mayer waves are of interest to researchers seeking to fully understand the functioning of the cardiovascular system. It is generally conceded that Mayer waves appear most often when the subjects are exposed to abnormal conditions. Lack of oxygen, the effects of severe haemorrhage, and other extreme or sudden changes in blood supply to parts of the body favour the appearance of these slow periodic fluctuations (Anderson *et al*., 1950). Experiments have shown that when the blood pressure is measured for subjects lying in a supine position and then in a tilted position, there may exist Mayer-like oscillations for the tilted position. A remarkable feature observed in these experiments is that the Mayer waves occur more frequently in younger subjects, and disappear with age (Epstein *et al.*, 1968; Kaplan *et al*., 1991; Miyamoto *et al*., 1982).

It is essential, for survival, that blood pressure be controlled to stay within a narrow, safe range. This function is performed by the body's control mechanisms, the fastest being the baroreflex. The baroreceptors are stretch sensors located in the systemic arteries which detect changes in blood pressure. The baroreflex feedback loops respond to baroreceptor impulses to control blood pressure via three mechanisms: heart rate, systemic capillary resistance and venous volume. All the three

mechanisms are explored in this work. DeBoer (Deboer *et al.,* 1987) proposed that blood pressure variability is caused by a time delay in the baroreceptor loop. If this were the case, one would expect the delay to increase with age due to a slowing of the body's responses. This would then cause an increase in the existence of Mayer waves in older people. While one does not discount the contribution of delay, it appears not to be the main cause of Mayer waves.

It is hypothesized that blood pressure variability may be attributed to a change in feedback gain, extending the work of (Wesseling *et al.,* 1982). Previous studies of feedback-control systems in physiology (Glass and Mackey, 1988; Langford, 1977), and in engineering (Hassard *et al.,* 1981), have shown that an increase in feedback gain can cause a system to change behaviour from a steady state to an oscillating state. This may be called a "gain-induced instability" and has been studied by use of the Hopf Bifurcation theory. Since young adult humans tend to have quicker reflexes and better muscle tone than the elderly, they can be expected to have higher gain in the baroreceptor loop. Thus our hypothesis that Mayer waves may be a gain-induced instability is consistent with the observed age-related data. A mathematical model can be used to give greater insights into the roles of the various mechanisms affecting Mayer waves. In addition to incorporating temporal dynamics, this model will allow investigation of the effects of each of the three baroreflex feedback loops, independently of the other two. Parameter values in the mathematical model are chosen to correspond to a typical adult human being.

The primary objective of this study is to develop a dynamical model for the mammalian circulatory system and use it to analyze blood pressure variability dynamics, as a function of the physiological parameters in the model. The model is used to establish the existence of Mayer waves and their disappearance with age.

The Model

While it is desirable to include the behaviour of each cardiovascular component in a model of the circulation, certain components can be lumped together without sacrificing the qualitative behaviour of the system (Avula *et al.,* 1978; Lipsitz and Goldberger, 1992). The modeling assumptions and the development of the model, first for the basic fluid flow of blood in the cardiovascular system, then with the nonlinear baroreflex control are stated below:

Assumptions

1. The cardiovascular system is a closed-looped hydrodynamic system comprising two heart pumps, two large arteries, two veins and the two capillary networks, corresponding to the systemic and pulmonary circulations respectively. The total blood volume is constant in time.
2. The large arteries and veins and the heart are compliance vessels (Anderson *et al.,* 1950), that is, volume is proportional to pressure in these vessels. On the other hand, the smaller arteries and veins in the capillary networks are resistance vessels, that is, flow is proportional to pressure. The unstressed volume of blood vessels is negligible at all parts of the circulation except in the systemic veins.
3. Flow from the heart is continuous, that is the pulsatile nature of blood pressure is neglected and only average pressures and volumes, over the period of the pulse, are dealt with.
4. The pressure in the heart when relaxed, is equal to that of the veins supplying blood to it.
5. The baroreceptor feedback gain and its dependence on systemic arterial pressure is modelled as a Hill function (described below).
6. Changes in venous volume, systemic resistance and heart rate act independently in parallel on blood pressure.
7. Compliance is constant in all parts of the cardiovascular system except the systemic veins, where it may be varied by the baroreflex.
8. Resistance is constant for the capillary networks of the pulmonary circulation, but may be varied by the baroreflex in the systemic circulation.

Model Development

A notational convention adopted throughout this model is that dynamic variables are represented by lower case letters, while parameters and labels are written in upper case. A simple linear model of the cardiovascular system is first constructed, then the baroreflex control system is added. Given that Q is concentration of blood and λ is a constant, Diagram shows the flow of blood from the heart to other parts of the body and back to the heart:
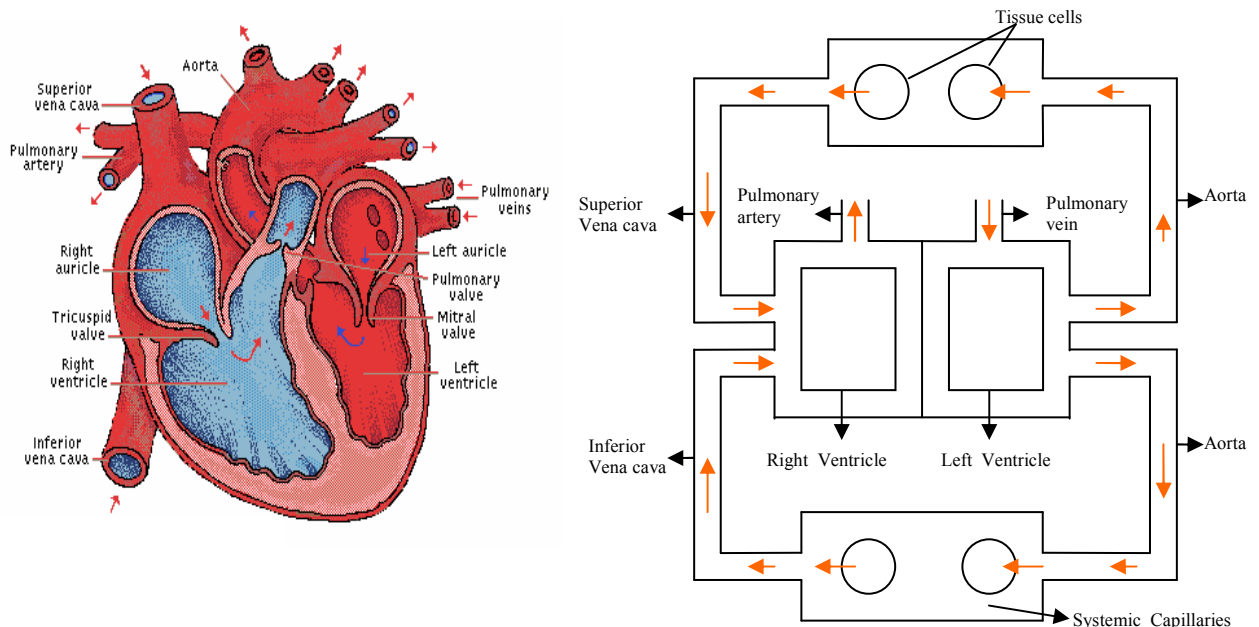
Figure 1: Diagrams showing the flow of blood in the heart.
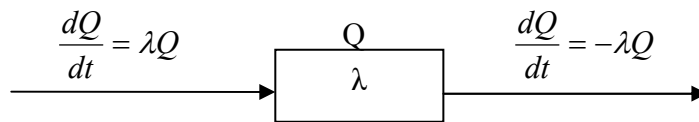
Linear Cardiovascular Model

The following linear relationship between volume, V, pressure, P and compliance, C, in the large vessels (arteries and veins) of the circulation (Hoppensteadt and Peskin, 1992), is the mathematical form of Assumption 2.

$$V = C \times P \tag{1}$$

There are four such equations in the model, corresponding to the systemic arteries and veins, and the pulmonary arteries and veins, for which the variables V, P, C are distinguished by subscripts SA, SV, PA, PV respectively. However, Equation (1) suggests that if P = 0, then V = 0, which is not the Case, especially in the systemic veins which typically contains about 70% of the blood in a human body. More realistic relations are:

$$V_{SA} = C_{SA} \times P_{SA} \tag{2}$$

$$V_{SV} = C_{SV} \times P_{SV} + V_D \tag{3}$$

$$V_{PA} = C_{PA} \times P_{PA} \tag{4}$$

$$V_{PV} = C_{PV} \times P_{PV} \tag{5}$$

where V_D is the unstressed volume, that is the volume of the vessels at p = 0. The unstressed volume in the systemic venous circulation is very important, as over one-half of the venous volume is unstressed volume (Coleman, 1985). However, the unstressed volume in the other three compliance vessels is neglected. The flow, q in the vessels of the capillary networks, modelled (Hoppensteadt and Peskin, 1992). as resistance vessels, is

$$q = \frac{P_A - P_V}{R} \tag{6}$$

Here P_A, P_V and R represent the pressure in the arteries and veins and resistance respectively, in either the systemic or pulmonary circulation. Thus there two such equations of the form (6), for systemic and pulmonary capillary flows, distinguished by the subscripts S and P respectively on all variables:

$$q_S = \frac{P_{SA} - P_{SV}}{R_S} \tag{7}$$

$$q_P = \frac{P_{PA} - P_{PV}}{R_P} \tag{8}$$

From the Frank-Starling Assumption 4, the following relations for the left and right cardiac outputs, q_L and q_R, respectively are given:

$$q_L = F \cdot C_L \cdot P_{PV} = K_L \cdot P_{PV} \tag{9}$$

$$q_R = F \cdot C_R \cdot P_{SV} = K_R \cdot P_{SV} \tag{10}$$

Here C_L and C_R are the compliances in the left and right hearts respectively and F is the heart beat frequency. The subscripts A and V represent arteries and veins respectively, while the subscripts S and P stand for the systemic and pulmonary circulations, respectively. The rate of change of volume of an incompressible fluid in a vessel is the difference between the rates of flow of the fluid, into and out of the vessel. Hence, the following differential equations are obtained, for the change of volume of blood in the systemic arteries, systemic veins, pulmonary arteries and pulmonary veins respectively:

$$\frac{dv_{SA}}{dt} = q_L - q_S \tag{11}$$

$$\frac{dv_{SV}}{dt} = q_S - q_R \tag{12}$$

$$\frac{dv_{PA}}{dt} = q_R - q_P \tag{13}$$

$$\frac{dv_{PV}}{dt} = q_P - q_L \tag{14}$$

q_L, q_R, q_S and q_P, represent flow through the left heart, the right heart, the systemic capillaries and the pulmonary capillaries, respectively. At this stage there are twelve equations with twelve unknowns: eight algebraic equations (1)-(10) and four differential equations (11) - (14). The eight algebraic equations may be used to eliminate the flow variables q and the pressure variables p from the system of differential Equations. The result is a system of four differential equations in the four volume variables. From Assumption 1, that blood is conserved, the following is obtained:

$$V_{SA} + V_{SV} + V_{PA} + V_{PV} = V_O \tag{15}$$

where V_O is the total blood volume, a constant. Equation (15) indicates that the four volume variables are not independent. As V_{PA} has the smallest value, it is chosen for elimination and a system of three

equations in V_{SA}, V_{SV} and V_{PV}, is obtained as follows (mathematically any one of the four volume variables could be eliminated).

Hence the mathematical model of the cardiovascular system consists of the following system of three ordinary differential equations.

$$\frac{dv_{SA}}{dt} = F \cdot C_L \cdot \frac{V_{PV}}{C_{PV}} - \frac{V_{SA}}{R_S \cdot C_{SA}} + \frac{V_{SV}}{R_S \cdot C_{SV}} - \frac{V_D}{R_S \cdot C_{SV}} \tag{16}$$

$$\frac{dv_{SV}}{dt} = \frac{V_{SA}}{R_S \cdot C_{SA}} - \left[\frac{1}{R_S \cdot C_{SV}} + \frac{F \cdot C_R}{C_{SV}} \right] [V_{SV} - V_D] \tag{17}$$

$$\frac{dv_{PV}}{dt} = \frac{V_O - V_{SA} - V_{SV} - V_{PV}}{R_P \cdot C_{PA}} - \left[\frac{1}{R_P \cdot C_{PV}} + \frac{F \cdot C_L}{C_{PV}} \right] \cdot V_{PV} \tag{18}$$

Note that this model is linear in the three volume variables represented by lower case V's. The system becomes nonlinear, on the inclusion of the baroreflex feedback control loops.

Model with Baroreceptor Control

The Hill function is defined by:

$$y = f_n(x) = \frac{x^n}{a^n + x^n} \tag{19}$$

The baroreceptor response curve described in the literature strongly resembles a Hill function and therefore is modelled in this thesis as:

$$B_n(P_{SA}) = \frac{(P_{SA})^n}{(P_C)^n + (P_{SA})^n} \tag{20}$$

where B_n is the total baroreceptor afferent activity, n is a measure of the baroreflex gain, and P_C, is the critical arterial pressure. The term "gain" normally is used to represent a ratio of the change in output to a change in input, for very small changes in B_n. This is however, essentially the mathematical definition of a derivative. The figure below shows the graph of the Hill function with n = 3 and P_C = 1 using TI 89.
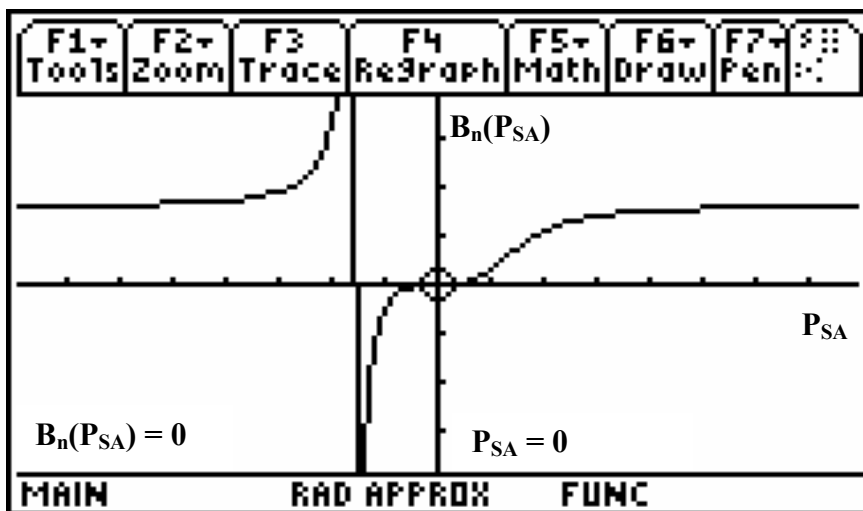
Figure 2: Graph of the Hill function

Thus, for our model, using the Hill function for the baroreflex response, the gain is defined by the derivative

$$\mu = \frac{dB_n}{dP_{SA}} \qquad (21)$$

Thus, this becomes

$$\mu = \frac{n(P_{SA})^{n-1} \cdot (P_C)^n}{\left[(P_C)^n + (P_{SA})^n\right]^2}$$

If $P_{SA} = P_C$

$$\mu = \frac{n}{4P_C} \qquad (22)$$

that is, gain μ is equal to the slope of the response function (for fixed n), at a particular point.

This is a good measure of the gain as it is very close to the maximum value of the slope. The variables are scaled so that $P_C = 1$, and μ $\mu = n/4$. Also, P_{SA} is proportional to V_{SA} (since C_{SA} is a constant), so B_n can be expressed in terms of V_{SA} rather than P_{SA}. This yields:

$$B_n(P_{SA}) = B_n\left(\frac{V_{SA}}{C_{SA}}\right) = \frac{(V_{SA})^n}{(V_C)^n + (V_{SA})^n} \qquad (23)$$

where V_C is the volume at the critical pressure. Changes in heart rate, F and systemic capillary resistance, R_S must be in an opposite direction to a change in arterial blood pressure, in order to restore normal pressure. Thus a simple model of the baroreflex action on F is:

$$F = F_O(1 - B_n) = \frac{F_O(V_C)^n}{(V_C)^n + (V_{SA})^n} \qquad (24)$$

where F_O is a constant. Equation (24) implies that if B_n approaches 1 (i.e. very large pressure P_{SA}), then F will be zero. However, one would expect that in reality F will have a non zero minimum value even when B_n approaches 1. The following is a more realistic representation:

$$F = F_1(1 - B_n) + F_2 = \frac{F_1(V_C)^n}{(V_C)^n + (V_{SA})^n} + F_2 \qquad (25)$$

where F_1 and F_2 are constants, and F_2 is the value of F when $B_n = 1$. Similarly, the baroreflex action on R_S is modelled as:

$$R_S = R_1(1 - B_n) + R_2 = \frac{R_1(V_C)^n}{(V_C)^n + (V_{SA})^n} + R_2 \qquad (26)$$

On the other hand, changes in systemic venous compliance, C_{SV}, and systemic venous unstressed volume, V_D, are in the same direction as a change in arterial blood pressure. Thus the action of the baroreflex on each of V_D and C_{SV} is modelled as:

$$V_D = D_1 \cdot B_n + D_2$$

or

$$V_D = \frac{D_1(V_{SA})^n}{(V_C)^n + (V_{SA})^n} + D_2 . \qquad (27)$$

Likewise,

$$C_{SV} = C_1 \cdot B_n + C_2$$

or

$$C_{SV} = \frac{C_1 (V_{SA})^n}{(V_C)^n + (V_{SA})^n} + C_2 \tag{28}$$

Now, from the basic linear cardiovascular model (16), (17) and (18), four different nonlinear cardiovascular models are obtained, corresponding to insertion of the baroreceptor feedback function into each of F, R_S, C_{SV} and V_D, as above. This allows independent investigations of each of the four feedback loops, which would be difficult and dangerous to carry out experimentally on live subjects.

Parameter Determination

Many of the parameters in this model are available in the literature, as displayed in Table 1. The remaining parameters, F_1, F_2, R_1, R_2, C_1, C_2, D_1, D_2, C_{SV}, V_C and V_D are not found in the literature and need to be determined.

Critical Volume, Vc

No value of V_C is in the literature. However the normal resting value of V_{SA} is known to be 1.0 litre. It is assumed that the resting and critical states are the same and hence V_C is taken as 1.0 litre. Since V_C plays the role of a in equation (22), this has the bonus effect simplifying the formula (22) for the gain, to $\mu = n/4$.

Table 1   Typical parameter values for an adult human being

PARAMETER	NORMAL VALUE
Compliance in Systemic Arteries, C_{SA}	0.01 litres/mm Hg
Compliance in Pulmonary Arteries, C_{PA}	0.00667 litres/mm Hg
Compliance in Pulmonary Veins, C_{PV}	0.08 litres/mm Hg
Systemic resistance, R_S	17.5 mm Hg/(litre/min.)
Pulmonary resistance, R_P	1.79 mm Hg/(litre/min.)
Compliance in Right Heart, C_R	0.035 litres/mm Hg
Compliance in Left Heart, C_L	0.014 litres/mm Hg
Heart rate, F	80 beats/min.

(Source: Hoppensteadt and Peskin, 1992)

Normal Systemic Venous Unstressed Volume, V_D

An exact normal value of V_D is not found in the literature. However, (Coleman, 1985), gives the value of V_D as "over half" the systemic venous volume V_{SV}. As the normal value of V_{SV} is 3.5 litres, the normal value of V_D is taken as 2.0 litres in this study.

Normal Systemic Venous Compliance, C_{SV}

The normal systemic venous compliance is given as 1.75 litres/mm Hg (Hoppensteadt and Peskin, 1992). This value of C_{SV} does not account for systemic venous unstressed volume. However, this study considers the systemic venous unstressed volume. Using Equation (3), with V_{SV} = 3.5 litres, V_D = 2.0 litres and P_{SV} = 2 mm Hg, the corresponding value of C_{SV} is computed as 0.75 litres/mm Hg.

Normalized Hill Function Constants, F_1, F_2, R_1, R_2, C_1, C_2, D_1, and D_2

These constants are required for the use of the Hill function to model the baroreceptor afferent activity, B_n, acting on the systemic venous compliance, systemic venous unstretched volume,

systemic resistance and heart rate. This current study appears to be the first time such an approach has been taken, hence the non-availability of these constants. Therefore, sets of different values of each of these constants are investigated in this study, over ranges which yield baroreceptor responses consistent with experimental observations.

Analysis and Discussion

Analysis

The control of the baroreflex on heart rate, F, systemic capillary resistance, R_S, systemic venous unstressed volume, V_D, and systemic venous compliance, C_{SV}, are investigated individually in the mathematical model. Specifically, the appropriate non-linear baroreflex response function, from (25) to (28) is substituted in each parameter in turn, to obtain the corresponding model for investigating the baroreflex effect on the parameter under consideration. Each of the four models is analyzed to find out if a bifurcation occurs as the baroreceptor gain μ varies, using Hopf's Bifurcation Theory.

First, the steady state solution of each model was found. Then the system of equations was linearised at this steady state. The value of the Jacobian matrix evaluated at the steady state was found. Since it is a real 3×3 matrix, with constant real entries, the eigenvalues are either all three real or else one real and two complex conjugate. The eigenvalues of the resulting matrix were also found. In each case there existed, for some values of μ, one real and two complex eigenvalues. The real part of the pair of complex conjugate eigenvalues was plotted as a function of μ, to find out if a crossing point existed. The value of μ at which the real part crosses the μ-axis is what is known as the crossing point or Hopf bifurcation point. At this point there exists a pair of purely imaginary eigenvalues ($\pm i$) and the steady state is said to be non-hyperbolic. When a crossing point was found, the imaginary part of the complex eigenvalues was plotted to obtain its value at the crossing point. The third (real) eigenvalue always remained negative. According to the general theory of Liapunov stability, when the real part of the complex eigenvalues crosses from negative to positive, the equilibrium state changes from asymptotically stable to unstable. The computation of the eigenvalues and the plotting of the curves were done using Mathlab. From the Hopf Bifurcation Theorem (Hassard *et al.,* 1981), generically at such a crossing point, a periodic solution is either created or destroyed. Further numerical computations verify the existence of a stable limit cycle near the crossing point. The imaginary part at the crossing point gives a good approximation to the frequency of the resulting oscillations.

Baroreflex Control of Heart Rate

Models with R_S, C_{SV} and V_D taken as constants and F given by Equation (25) were considered.

$V_C = 1$ and $V_{SA} = 1$. Then $F = \dfrac{F_1}{2} + F_2$

Assuming a normal heart rate of 80 beats/min., values of F_1 and F_2 considered were: F_1 = 160 beats/min. and F_2 = 0 beats/min., F_1 = 80 beats/min. and F_2 = 40 beats/min., and F_1 = 40 beats/min. and F_2 = 60 beats/min. All of these models exhibited a stable steady-state, for all values of gain μ tested. No evidence of waves was found, (Abbiw-Jackson, 1997) as shown in Figure 3.
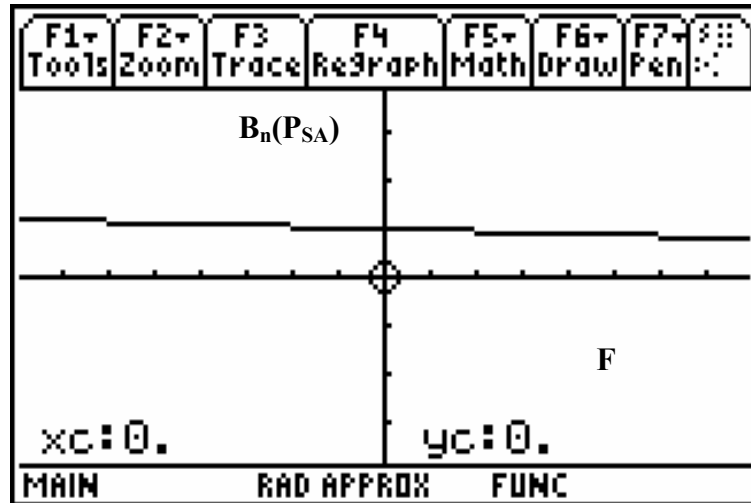
Figure 3   **Graph of Baroreflex action on changes in heart rate, F, using TI 89**

Baroreflex Control of Systemic Resistance

Models with the baroreflex affecting only systemic resistance R_S, while C_{SV}, V_D and F are taken as constants, are considered next. R_S is given by Equation (26) and a typical value of systemic resistance is 17.5 mmHg/(litre/min.).

$$R_S = \frac{R_1}{2} + R_2$$

Values of R_1 and R_2 used are: $R_1 = 35$ mm Hg/(litre/min.) and $R_2 = 0$ mm Hg/(litre/min.), $R_1 = 20$ mm Hg/(litre/min.) and $R_2 = 7.5$ mm Hg/(litre/min.), and $R_1 = 15$ mm Hg/(litre/min.) and $R_2 = 10$ mm Hg/(litre/min.). These models had a stable steady-state for all values of gain, μ tested, and showed no indications of waves (Abbiw-Jackson, 1997), as shown in Figure 4.
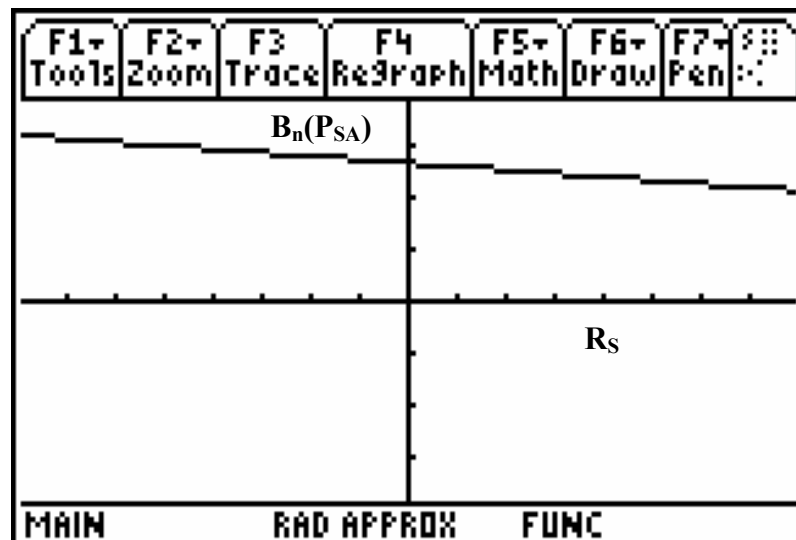
Figure 4   **Graph of Baroreflex action against Resistance, R_S, using TI 89**

Baroreflex Control of Venous Volume

The baroreflex influences the systemic venous volume through the unstressed volume, V_D and the compliance, C_{SV}. Models with the baroreflex controlling C_{SV} and V_D individually were considered. For both cases the models exhibited unstable steady-states for gains past a crossing point with pure imaginary eigenvalues. Figures (5 to 8) display four graphs obtained for models with the baroreflex controlling unstressed venous volume. It shows graphs of the real parts of the complex eigenvalues, for models with D_2 equal to 0, 0.5, 1.0, and 1.5 litres, respectively. Note that Re(λ) crosses through zero in all cases. This implies a Hopf bifurcation, giving birth to an oscillation or wave.

Similarly, Figures (9 to 11) are obtained from models with the baroreflex controlling venous compliance only. It shows graphs of the real parts of the complex eigenvalues for three cases of models with C_2 equal to 0, 0.25, and 0.5 litres/mm Hg, respectively. All three cases give a Hopf bifurcation. The values of the imaginary parts of the complex eigenvalues at the crossing points give the angular frequency of the oscillations produced.

Control of Venous Volume

The mathematical model has been constructed so that the systemic venous unstressed volume V_D is controlled by the baroreflex, while R_S, C_{SV} and F are assumed to remain constant. The explicit effect on V_D of the baroreflex is given by Equation (27). Different choices of the constants D_1 and D_2 in (27) were considered. The stability of the equilibrium state is investigated, by computation of the eigenvalues of the Jacobian matrix, using Mathlab, in exact rational arithmetic. The results presented here are expressed in terms of exact rational numbers, free of the round off errors which would be introduced by finite decimal representations.

$D_1 = 4.0$ litres and $D_2 = 0$ litres

Using equations (16), (17), (18), we obtain the system of equations representing the circulation for each set of values for D_1 and D_2 as follows:

$$\frac{dV_{SA}}{dt} = -\left(\frac{40}{7}\right)V_{SA} + \left(\frac{8}{105}\right)V_{SV} + 14V_{PV} - \left(\frac{32}{105}\right)\left[\frac{(V_{SA})^{4\mu}}{1+(V_{SA})^{4\mu}}\right]$$

$$\frac{dV_{SV}}{dt} = \left(\frac{40}{7}\right)V_{SA} - \left(\frac{80}{21}\right)V_{SV} + \left(\frac{320}{21}\right)\left[\frac{(V_{SA})^{4\mu}}{1+(V_{SA})^{4\mu}}\right]$$

$$\frac{dV_{PV}}{dt} = 420 - 84V_{SA} - 84V_{SV} - 105V_{PV}$$

The steady state values of the system are found to be: $V_{SA} = 1.0$ litres, $V_{SV} = 3.5$ litres, and $V_{PV} = 0.4$ litres. Linearization of the model at the steady state gives the matrix A.

$$A = \begin{pmatrix} \dfrac{-40}{7} & -\dfrac{32\mu}{105} & \dfrac{8}{105} & 14 \\ \dfrac{40}{7} & \dfrac{320\mu}{21} & \dfrac{-80}{21} & 0 \\ & -84 & -84 & -105 \end{pmatrix}$$

The eigenvalues of A are:

$$\lambda_1 = U^{\frac{1}{3}} - V - \frac{2405}{63} - \frac{32\mu}{315}$$

$$\lambda_2 = \frac{U^{\frac{1}{3}}}{2} + \frac{V}{2} - \frac{2405}{63} - \frac{32\mu}{315} + \frac{i}{2}\sqrt{3}(U^{\frac{1}{3}} + V)$$

$$\lambda_3 = \frac{U^{\frac{1}{3}}}{2} + \frac{V}{2} - \frac{2405}{63} - \frac{32\mu}{315} - \frac{i}{2}\sqrt{3}(U^{\frac{1}{3}} + V)$$

where

$$U = \frac{-5103633725}{250047} - \frac{3618065648\mu}{416745} + \frac{184832\mu^2}{416745} - \frac{32768\mu^3}{31255875} +$$

$$\frac{8}{2835}(4488999170550 + 45082290017400\mu + 9458754238932\mu^2$$

$$- 942218496\mu^3 + 2248704\mu^4)^{1/2}$$

$$V = U^{-\frac{1}{3}}\left(\frac{-2876953}{3969} + \frac{11552\mu}{3969} - \frac{1024\mu^2}{99225}\right)$$

For values of μ of interest, eigenvalue λ_1 is real and negative. Eigenvalues λ_2 and λ_3 are complex conjugates, with real part which crosses through zero from negative to positive as μ increases, near μ = 18, as shown in the figure below:
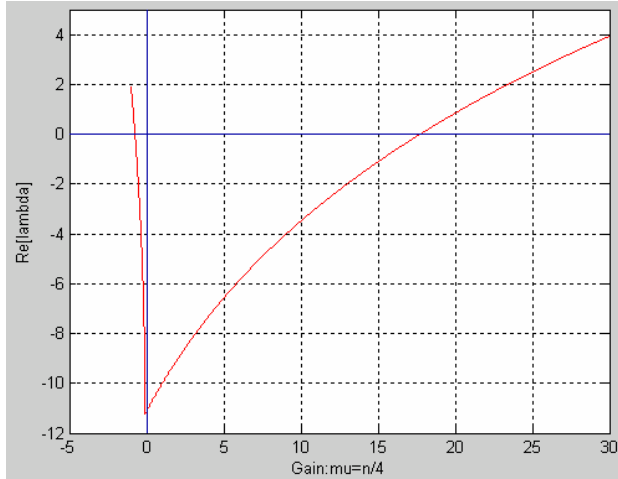
Figure 5: Re(λ) as a function of μ for controlled V_D with D_2 = 0 litres.
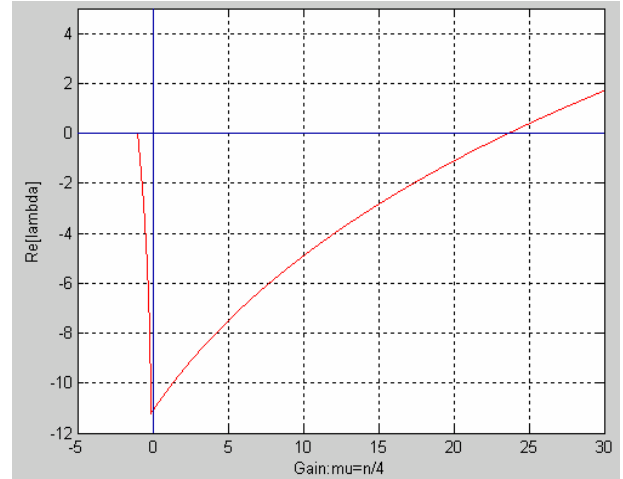
Figure 6: Re(λ) as a function of μ for controlled V_D with D_2 = 0.5 litres
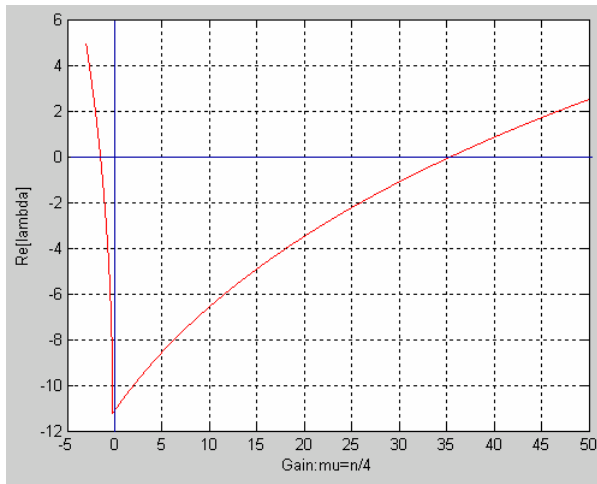
Figure 7: Re(λ) as a function of μ for controlled V_D with D_2 = 1.0 litre
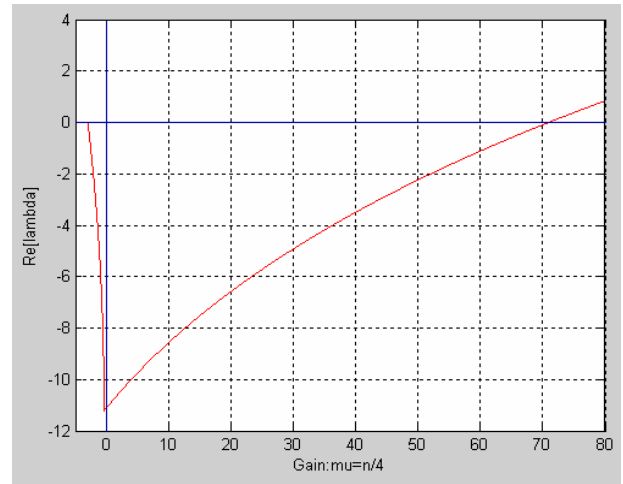
Figure 8: Re(λ) as a function of μ for controlled V_D with D_2 = 1.5 litres

Control of Venous Compliance

A mathematical model is constructed in which the systemic venous compliance C_{SV} is controlled by the baroreflex, while RS, V_D and F, are held constant. C_{SV} is given by Equation (28). The stability of the model, for different values of C_1 and C_2 is explored. The results of these calculations are presented in Figure (9 to 11).
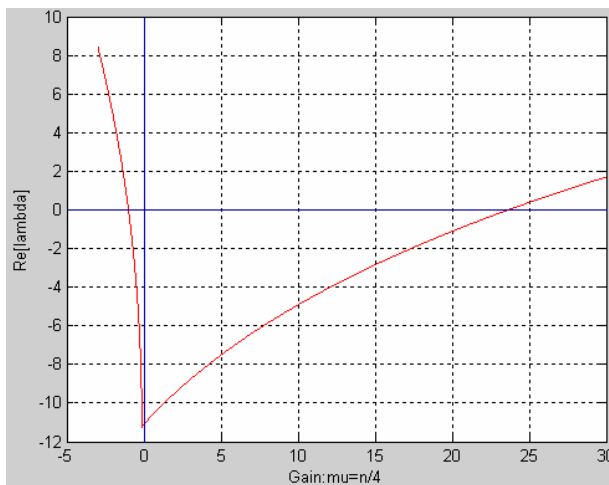
Figure 9: Re(λ) as a function of μ for controlled Csv with C_2 = 0 litres/mm Hg.
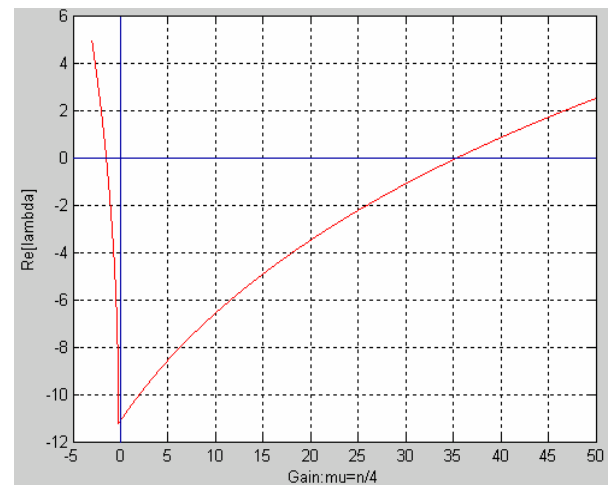
Figure 10: Re(λ) as a function of μ for Controlled Csv with C_2 = 0.25 litres/mmHg.
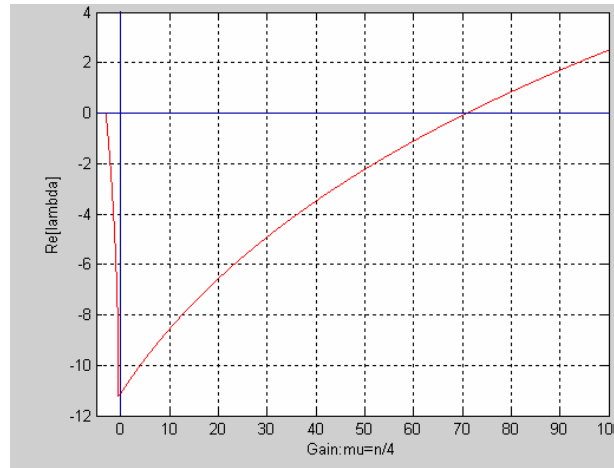
**Figure 11: Re(λ) as a function of μ for
controlled Csv with C₂ = 0.5 litres/mm Hg.**

Discussion

Models with only heart rate F, or systemic capillary resistance R_S, controlled by the baroreflex did not exhibit a Hopf Bifurcation, while the models with systemic venous compliance, C_{SV} or systemic venous unstressed volume, V_D controlled by the baroreflex were capable of Hopf bifurcation. Hence the effect of the baroreflex on F and R_S, individually, is not the cause of oscillations. However, if the effect of the baroreflex on F and R_S were combined in models with the effects on V_D or C_{SV}, they may play a part in causing instability.

It is observed that for all models with V_D and C_{SV} individually controlled by the baroreflex, the real part of the complex eigenvalues increases as the gain, μ, increases and the graph crosses the μ-axis at a positive value of μ. This implies a Hopf bifurcation and the presence of a limit cycle oscillation. The stability of this limit cycle oscillation has been verified numerically. The similarity of the results obtained for models with C_{SV} and V_D individually controlled by the baroreflex is to be expected, as the two have similar effects on blood flow. The model with the baroreflex controlling only C_{SV} is more stable than that with the baroreflex controlling only V_D. Thus it appears that the baroreflex control of V_D is more important than the control of C_{SV} where gain induced instability is concerned, but control of C_{SV} also plays an important part.

Further insights were obtained on varying two parameters in the model simultaneously; namely, the gain parameter μ together with either one of D_2 or C_2 (the minimum unstressed systemic venous volume or compliance respectively). As either of D_2 or C_2, increases, the value of gain at which the graph crosses the μ-axis increases. This suggests that an increase in D_2 or C_2 increases the stability of blood pressure. Changing the value of D_2 or C_2 causes re-setting of the baroreceptor curve. However as different people may have different D_2 and C_2 values, different people can be expected to take different times before Mayer waves are observed, when subjected to identical Mayer wave inducing stresses. In particular it could be expected that young and old people will have different D_2 and C_2 values and this may explain the difference in the incidence in Mayer waves observed in young and old people. As one would expect, larger D_2 and C_2 values in older people, correspond to veins which have become stretched and less fit.

In Figure 12, D_2 is plotted against the crossing point value of gain μ. The top left region represents the parameter values for which the equilibrium state is stable, and corresponds to older subjects, who would tend to have smaller gains μ, and larger D_2 values. The lower right region represents unstable equilibria, susceptible to oscillations, and corresponds to youth. Thus, stability depends on both the baroreflex gain μ and D_2. Thus, young adults, with high gain and small D_2, are in the unstable region, while older adults with the opposite characteristics are in the stable region. A similar situation holds for μ and C_2. The conclusion is that the existence of Mayer waves and their disappearance with age can be explained, at least in part, as a case of gain induced instability.

Venous Dead Volume Vs Gain
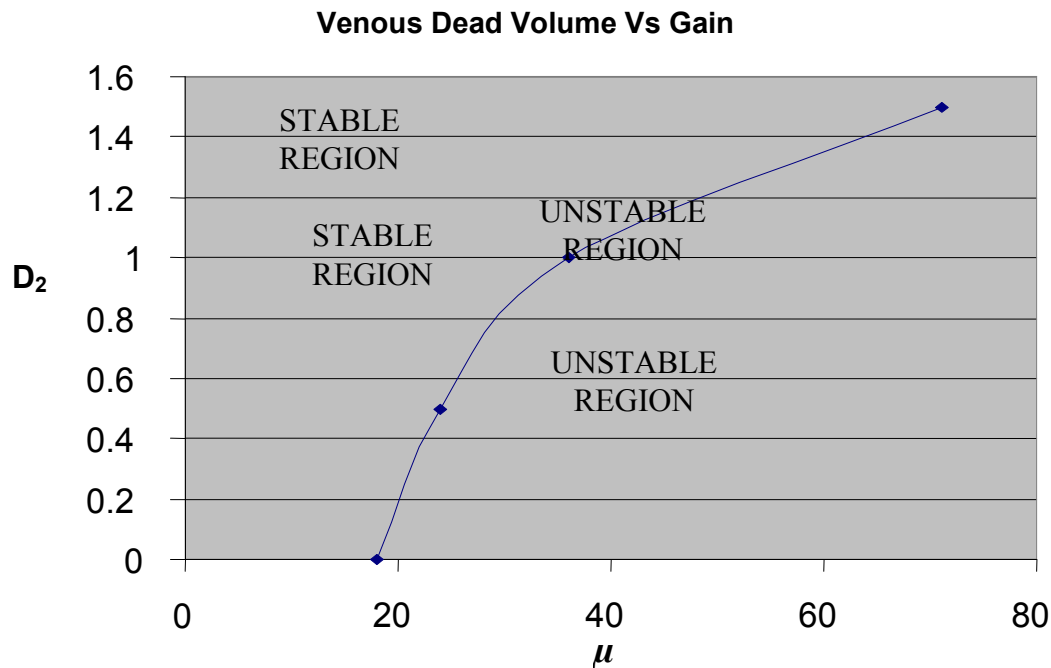
Figure 12:   Graph of D_2 against crossing point values of μ

Conclusions

A simple model for the human cardiovascular system with baroreceptor control feedback has been proposed. The model has been reduced to a single delay-recruitment equation, and the behaviour of solutions have been studied analytically and numerically. Steady solutions can lose stability in a Hopf bifurcation to oscillatory solutions, consistent with Mayer waves, as delays are increased, or as feedback gain is increased, or as peripheral resistance is reduced. Chaotic dynamics are not a feature of our model.

The model indicates that sympathetic control of peripheral resistance is more important than sympathetic control of heart rate, and that solution stability is more sensitive to delay than to gain. The consequences of ageing are considered and found to be consistent with our model, with decreased gains giving more stable behaviour. Thus the principal conclusion of this paper is that the existence of Mayer waves and their disappearance with age may be explained by means of the Hopf bifurcation theorem, as a case of gain induced oscillations.

References

Abbiw-Jackson, R. M. (1997). Gain Induced Instability in Blood Pressure. University of Guelph, Canada.

Anderson, B. A., Kenney, R. A. and Neil, E. (1950). The role of the chemoceptors of the carotid and aortic regions in the production of the Mayer waves. Acta. physiol. scand. 20: 203-220.

Avula, X. A. J. and Ostreicher, H. L. (1978). Mathematical model of the cardiovascular system under acceleration stress. Aviat. Space Environ. Med. 49: 279-286.

Coleman, T.G. (1985). Mathematical analysis of cardiovascular function. IEEE Trans. Biomed. Eng. 32: 289-294.

Deboer, R. W., Karemaker, J. M. and strackee, J. (1987). Hemody- namic fluctuations and baroreflex sensitivity in humans: a beat to beat model. Am. J. Physiol . 253: H680-689.

Epstein, S. E., Stampfer, M. and Beiser, G.D. (1968). Role of the capacitance and resistance vessels in vasovagal syncope. Circulation. 37:524-533.

Glass, L. and Mackey, M. C. (1988). From Clocks to Chaos: The Rhythms of Life. New Jersey: Princeton University Press.

Hassard, B. D. Kararinoff, N. D. and Wan, Y. H. (1981). Theory and Applications of Hopf Bifurcation. Cambridge University Press.

Hoppensteadt, F. C. and Peskin, C.S. (1992). Mathematics in Medicine and the Life Sciences. New York: Springer-Verlag.

Kaplan, D. T., Furman, M. I., Pincus, S. M., Ryan, S. M., Lipsitz, L. A. and Goldberger, A. L. (1991). Aging and the complexity of cardiovascular dynamics. *Biophysical Journal 59, 945–949.*

Langford, W. F. (1977). Numerical solution of bifurcation problems for ordinary differential equations. Numer. Math. 28: 171-190.

Miyamoto, Y., Higuchi, J. and Mikami, T. (1982). Cardiorespiratory dynamics during vasovagal syncope induced by a head-up tilt. Japan J. Physiol . 32: 885-889.

Penaz, J. Mayer Waves, (1978). History and methodology. Automedica. 2: 135-141.

Wesseling, K. H. and Settels, J. J., Walstra, G., Van esch, H. J. and Donders, J. H. (1982). Baromodulation as the cause of short term blood pressure variability. World Scientific, p. 247-276.